Microencapsulation and controlled release of α-tocopherol by complex coacervation between pea protein and tragacanth gum: A comparative study with arabic and tara gums

Jérémy Carpentier, Egle Conforto, Carine Chaigneau, Jean-Eudes Vendeville, Thierry Maugard

Microencapsulation and controlled release of α-tocopherol by complex coacervation between pea protein and tragacanth gum: a comparative study with arabic and tara gums.

Jérémy CARPENTIER [a,c], Egle CONFORTO [b], Carine CHAIGNEAU [c], Jean-Eudes VENDEVILLE [c], Thierry MAUGARD [a]

[a] Université de La Rochelle, UMR CNRS 7266, LIENSs, UFR Sciences, Avenue Michel Crépeau, 17042 La Rochelle, FRANCE

[b] Université de La Rochelle, UMR CNRS 7356, LaSIE, UFR Sciences, Avenue Michel Crépeau, 17042 La Rochelle, FRANCE

[c] IDCAPS, filiale R&D INNOV'IA, 4 rue Samuel Champlain, Z.I. Chef de Baie, 17000 La Rochelle, FRANCE

*Author to whom correspondence should be addressed

E-mail: thierry.maugard@univ-lr.fr

Phone: +33 5 16 49 82 77

Key Words

Microencapsulation, Spray drying, complex coacervation, pea protein isolate, tragacanth gum, α-tocopherol

Abstract

The ability of pea protein isolates (PPI) to form complex coacervates with tragacanth gum was used for the microencapsulation of α-tocopherol mixture with pH-dependent release properties. The microcapsules were compared to three other models: PPI alone, PPI and gum arabic (PPI-GAC, known to form microcapsules of complex coacervates), and PPI and tara gum (PPI-TARA, non-ionic polysaccharides). The behaviors of the complex coacervates and microcapsules were studied according to the protein/polysaccharide mixture and protein/polysaccharide ratio. The formation of complex coacervates from the PPI-TRAG and PPI-GAC mixtures impacted the particle size of the liquid suspensions and microcapsules, the efficiency of encapsulation and the active release profile. An interesting gastroprotective behavior was identified for the PPI-TRAG mixture at the 1:1 ratio in simulated digestion media. Overall, the results showed the ability of PPI associated with polysaccharides to form microcapsules with a pH-dependent release behavior, that is promising in the field of gastroprotective microencapsulation.

1. Introduction

α-tocopherol, the major form of vitamin E, is a biologically active hydrophobic antioxidant widely used to reduce the risk of cardiovascular diseases (Pryor, 2000; Yang & McClements, 2013). Although α-tocopherol is beneficial to human health, its poor hydrosolubility and relative sensitivity to light, heat and oxygen limit its bioavailability and its applications in food, pharmaceutical and cosmetic fields (Chen et al., 2013; Chiu & Yang, 1992). Therefore, encapsulation is needed for its protection and targeted release in the digestive system.

Microencapsulation is an effective technology used to protect biologically active compounds against environmental factors (light, humidity, oxidation process, chemicals, volatile loses), and also to increase their solubility and bioavailability. Microencapsulation involves the formation of a protective shell to encapsulate the sensitive compound or embed it in a matrix material (Sobel et al., 2014). Among the microencapsulation techniques used in food industry, complex coacervation and spray drying may be cited. Complex coacervation is an effective method for lipophilic active compounds microencapsulation due to high payload, high encapsulation efficiency and mild processing conditions. Complex coacervation consists in forming coacervates from the electrostatic interaction of two oppositely charged biopolymers on the surface of the active compound at a specific condition of pH, temperature and ionic strength (Timilsena et al., 2016). The process includes four main steps: emulsification, coacervation, reticulation (optional) and drying. The complex coacervate -based shells provide microcapsules using emulsification followed by spray-drying with good stability (Barrow et al., 2007). The process prevents the migration of oil to the particle surface and gives greater protection to encapsulated omega-3-oil (Eratte et al., 2014). Complex coacervation has been reported as an effective method for the microencapsulation of lipophilic active compounds (fish oil), using a gelatin/polyphosphate mixture as an encapsulating matrix (Barrow et al., 2007). Gelatin has also proven its efficacy as a cationic compound associated with polyanionic compounds such as gum arabic, pectin, carboxymethylcellulose or alginate in the formation of complex coacervation systems encapsulating lipophilic compounds (Devi et al., 2012; Dong et al., 2011; Duhoranimana et al., 2018; Muhoza et al., 2019). The mechanism implies the interaction between the negatively charge polysaccharide and positively charged proteins below their isoelectric point. However, due to the emergence of new diseases in recent years, in particular prion-related diseases, health and safety regulations have been strengthened, leading to the use of different biopolymer sources (Chourpa et al., 2006). Consequently, proteins extracted from plant sources, especially from vegetables, have been widely developed in the food industry (Bajaj et al., 2017). However, the development of alternative protein-polysaccharide complex coacervates requires optimization of complex coacervation parameters because each protein-polysaccharide couple is able to form complex coacervate at a specific pH value and biopolymer mixing ratio that cannot be replicated to another set of biopolymers (Timilsena et al., 2017). Considerable research has been carried out using plant proteins such as soy, pea, lentil, chia seed proteins to microencapsulate oil (Ducel et al., 2004; Jun-xia et al., 2011; Liu et al., 2010; Timilsena et al., 2016). Among these plant proteins, pea proteins isolate (PPI) present a high nutritional value, non-allergenic properties, are rich in essential amino acids such as lysine, and have shown emulsifying and wall forming properties suitable for microencapsulation (Donsì et al., 2010; Ducel et al., 2005; Roy et al., 2010).

Tragacanth gum, described as a bifunctional emulsifier, showed efficient acidic oil-in-water emulsions properties (Balaghi et al., 2010; Farzi et al., 2013), gelling abilities and high mucoadhesive properties (Nur et al., 2016). Largely studied in biomedical field, tragacanth gum was identified as non-toxic, non-teratogenic, non-carcinogenic and non-mutagenic, and can be suitable in wound dressing (Ghayempour et al., 2016). Tragacanth gum forms complex coacervates with casein to

efficiently microencapsulate β-carotene (Jain et al., 2016). However, the complex coacervation of tragacanth gum associated with plant proteins is poorly described in the literature and might be consider as an alternative to the widely described gelatin-gum arabic system. Tragacanth gum is an anionic polysaccharide which remains negatively charged for a wide pH range, while pea proteins becomes positively charged below their isoelectric point (pI = 4,5-5.0) (Carpentier et al., 2021; Cuevas-Bernardino et al., 2018). Under specific conditions, these oppositely charged biopolymers interact with each other in aqueous solution to form complex coacervates. Because of its stability to acidity, tragacanth gum might be used as a gastroprotective biopolymer (Nazarzadeh Zare et al., 2019).

The general objective of this study is to develop a microencapsulation system with pH-dependent properties from plant biopolymers to encapsulate a lipophilic active compound model. Especially, the aim of this study was to develop microcapsules of complex coacervates from a mixture between pea protein isolates (PPI) and tragacanth gum to combine emulsifying properties of PPI, the pH-dependent behavior of protein-polysaccharide complex coacervates and the stability in acid media of tragacanth gum for the pH-dependent release of the encapsulated compound. The model was compared with the association of other polysaccharides (gum arabic or tara gum) at different ratios, according to the optimal parameters determined in a previous study and compared to microcapsules produced from PPI alone used as a vector of a hydrophobic active ingredient (Carpentier et al., 2021). A sunflower oil/α-tocopherol (90:10) (m/m) mixture was used as an active compound model for the active ingredient to be encapsulated. By varying the protein/polysaccharide ratio, the contribution of each biopolymer was assessed to understand the functionality of the complex coacervates and in particular their pH stability. The formulation conditions of the microcapsules produced at the pilot scale were adapted from a previous work for production purposes. In this context, the different formulations produced during the emulsion and coacervation process in liquid phase (by granulometric monitoring) and the microcapsules produced after drying were characterized, with a physical characterization of the microcapsules and encapsulation efficiency, of the particle morphology by scanning electron microscopy (SEM) and a study of the release of α-tocopherol in buffered and simulated digestion media.

2. Material and methods

2.1. Material and chemicals

The major pea storage proteins of the globulin family are legumin (350-400 kDa) and vicilin (150 kDa). Commercially available PPI (80% of protein content) in powder form were purchased from Roquette (Nutralys F85M, Lestrem, FRANCE). The product composition was described as follows: 7% of relative humidity, 80% of proteins, 3% of carbohydrates, 6% of total fat and 4% of ashes. The pea proteins were used without hydrolyzing. Gum arabic was kindly supplied by Nexira (Rouen, FRANCE). Tragacanth gum CEROTRAG 887 was purchased from C.E. Roeper GmbH (Hamburg, GERMANY). Tara gum is a galactomannan extracted from the endosperm of tara shrub (*Caesalpinia spinosa)* seeds. Tara gum was purchased from Starlight Products (Rouen, FRANCE). The gum obtained included ≥80% of galactomannan. All chemicals used in this study were of reagent grade and purchased from Sigma-Aldrich (Oakville, ON, Canada). Chloroform and acetonitrile used for α-tocopherol extraction and quantification, respectively, were purchased from Carlo Erba.

2.2. Preparation of sunflower oil supplemented with α-tocopherol and biopolymer stock solutions

Biopolymer dispersions (PPI, GAC, TRAG or TARA) of varying concentrations were prepared by adding a known amount of PPI, gum arabic (GAC), tragacanth gum (TRAG) or tara gum (TARA) powders in distilled water using an IKA RW20 Digital paddle stirrer (IKA, Staufen, Germany) (**Table 1**). Tragacanth gum and tara gum were hydrated at 45°C for 2 hours.

The active compound model consisted in a 90:10 mixture of sunflower oil and α-tocopherol prepared by adding a known amount of α-tocopherol to sunflower oil under magnetic stirring.

2.3. Preparation of Oil-in-Water (O/W) emulsions

PPI alone and the hydrophobic active mixture were pre-homogenized for 5 minutes at 5,000 rpm using the Ultra-Turrax (IKA, Staufen, Germany), and then further homogenized using a two-step MG2-500B homogenizer (BOS Homogenisers, Hilversum, Holland) at 250 bars for two cycles (**Table 1**).

2.4. Preparation of complex coacervates between the emulsion and polysaccharides

The process consisted in inducing coacervation between proteins and polysaccharides (**Table 1**). Briefly, the polysaccharide solution was added to the emulsion under deflocculant paddle stirring at 500 rpm for 10 minutes to limit the introduction of air into the mixture. The pH was then adjusted with 1M hydrochloric acid (HCl) under the optimal conditions of complex coacervation indicated in **Table 1**. A pH value corresponding to the highest complex coacervation was selected for a given ratio for each PPI-polysaccharide selected according to ζ-potential and coacervation yields studied in a previous work (Carpentier et al., 2021). Stirring was maintained during this step and continued for 10 minutes after addition of HCl, prior to the spray-drying of the suspension.

In the case of the emulsion of PPI alone, the pH was maintained at 6.8 after the high-pressure homogenization step. The aim of the study was to compare the properties of PPI microcapsules at the initial step to those from protein-polysaccharides complexes after acidification.

Table 1: Composition of the formulations of α-tocopherol microcapsules

Matrices	Ratio	pH	Active mixture (w/w) (%)	α-tocopherol (w/w) (%)	Matrix (w/w) (%)	Dry matter (%)
PPI	-	6.8	25.0%	2.5%	75.0%	5.0%
PPI-GAC	1:1	3.0	25.0%	2.5%	75.0% (37.5% of PPI – 37.5% of GAC)	5.0%
	2:1	3.5	25.0%	2.5%	75.0% (50% of PPI – 25% of GAC)	5.0%
	5:1	4.2	25.0%	2.5%	75.0% (62.5% of PPI – 12.5% of GAC)	5.0%
	10:1	4.4	25.0%	2.5%	75.0% (68.2% of PPI – 6.8% of GAC)	5.0%
PPI-TRAG	1:1	3.0	25.0%	2.5%	75.0% (37.5% of PPI – 37.5% of TRAG)	5.0%
	2:1	3.2	25.0%	2.5%	75.0% (50% of PPI – 25% of TRAG)	4.7%
	5:1	3.8	25.0%	2.5%	75.0% (62.5% of PPI – 12.5% of TRAG)	5.0%
	10:1	4.2	25.0%	2.5%	75.0% (68.2% of PPI – 6.8% of	5.0%

					TRAG)	
PPI-TARA	5:1	4.5	25.0%	2.5%	75.0% (62.5% of PPI – 12.5% of TARA)	4.5%
	10:1	4.5	25.0%	2.5%	75.0% (68.2% of PPI – 6.8% of TARA)	5.0%

2.5. Spray drying of complex coacervates in suspension

The spray-drying technology was used to prepare microparticles from feed solutions, composed of complex coacervates between PPI and polysaccharides. Suspensions were spray-dried using a Niro Minor pilot scale spray dryer (Niro Atomizer, Copenhagen, Denmark), equipped with a F11 turbine in order to obtain individualized microcapsules. The suspensions were fed into a drying chamber using a Masterflex Easy-Load II peristaltic pump (Cole Parmer, Montreal, Canada). The solutions were fed into an atomizing chamber with an inlet temperature of 140 ± 2°C and a flow rate of 400 kg/h. The outlet temperature was controlled between 75 and 80°C by adjusting the feed rate. The rotation frequency of the turbine was set at 50 Hz. Microcapsule powder was collected from the container, closed hermetically in opaque packaging and stored at 4°C until analysis. All experiments were performed in duplicate.

The spray-drying yield (SDY) was determined as follows:

$$SDY = \frac{m_f}{m_i} \times 100$$

Where m_f is the mass of collected powder and m_i is the initial mass of solid content added to the emulsion, including PPI, polysaccharides (GAC, TRAG or TARA) and the hydrophobic active mixture.

2.6. Particle size distribution of complex coacervates in suspension

Size distribution of emulsion oil droplets or suspensions of complex coacervates was estimated using a Malvern Mastersizer 3000 laser particle size analyzer (Malvern Instruments, Worcestershire, UK) equipped with a Hydro SM liquid feed unit. The particle size detected by the instrument ranged from 0.1 µm to 1,000 µm. The refractive indices used for particle size calculation were $\eta_{particle}$=1.456 and η_{water}=1.33. As the particle size distribution of the dispersions was multimodal, the results for each particle population were expressed according to the statistical parameter "mode" corresponding to the most represented value for this population. The percentage of each population was also estimated for a multimodal distribution.

2.7. Moisture content

The moisture content of formulated microcapsules was measured using a Halogen Moisture Analyzer HC103 (Mettler Toledo, Switzerland). Briefly, 2 g of powder were placed in an aluminum pan and heated at 105°C. Moisture content was measured for each sample after obtaining a stable weight. Tests were performed in duplicate and the mean values were expressed as a relative humidity percent (%RH).

2.8. Particle size distribution of microcapsules

The mean diameter of the spray-dried microparticles was determined by laser diffraction using a Malvern Mastersizer 3000 analyzer (Malvern Instruments, Worcestershire, UK) equipped with an Aero S dry powder feeder unit. The device operates based on the principle of multi-angular

diffraction of the laser red light at 633 nm. Briefly, about 2 g of microparticles were placed in the hopper of the device and the measurement was performed using a refractive index of 1.45 and the "fine particle" mode was activated to improve measurement (air pressure set at 2.5 bars). The measurement was recorded within the range from 0.1 to 1000 µm. From the size distribution, the volume diameter D (V; 0.5) and the dispersion of the data distribution curve (span) of the microparticles were determined by the software (Malvern). The volume particle diameter was calculated as the mean of two measurements per sample.

2.9. Fourier transform infrared (FTIR) spectroscopy

FTIR spectroscopy was used to investigate the functional groups of the spray-dried samples, biopolymer powders (proteins and polysaccharides) and hydrophobic active mixture. FTIR spectra were recorded using a Spectrum 100 FT-IR spectrometer (Perkin Elmer, Waltham, USA). Transmission spectra were obtained within a range from 650 to 4000 cm^{-1} using 32 scans at a resolution of 4 cm^{-1}. The scattering correction procedure was used for baseline correction of the spectra. Mean spectra were calculated from independent measurements performed in triplicate.

2.10. ESEM morphological observations

The morphology of the sample surface was monitored using an environmental scanning electron microscope (ESEM) (QUANTA 200 Environmental Field Effect Gun apparatus, FEI/ Thermo Fischer Scientific, USA). Observations were performed according to the method developed by Conforto *et al.* with some specifications (Conforto et al., 2015). The particles were deposited on conductive carbon double-faced adhesive tape on aluminum SEM stubs. As described by the author, no coating was applied to the samples before observation to avoid any alteration of the particle surface. The analyzes were performed in environmental mode under water vapor pressure with a beam current of 0.1 nA and an accelerating voltage of 11 kV. Secondary electron (SE) images were obtained using a large-field detector (LFD). Details of the surface morphology were obtained by adapting the water vapor pressure at 1.30 mbar. The value was suitable for the analysis of all samples under the chosen voltage and current conditions.

2.11. Quantification of α-tocopherol

100 mg of microcapsules (with an initial theoretical concentration of 2,5% of α-tocopherol (w/w)) were suspended in 4.5 mL of chloroform in a vial. The solution was stirred vigorously for 10 minutes. 1 mL of the chloroform phase was removed and centrifuged for 10 min at 12,000 rpm. The supernatant was diluted by two in acetonitrile and stored in a sealed vial for HPLC analysis.

A standard curve with known concentrations of α-tocopherol ranging between 0.1 and 1000 µg/mL was used. α-tocopherol concentration was estimated by calculating the area under the UV detection peak after HPLC separation.

α-tocopherol concentration in the samples was measured using a HPLC system (Agilent) equipped with an Uptisphere C18 WOD column (Interchim) and an UV-Vis detector (Agilent). The compound was eluted in a mobile phase consisting in a mix of water (5%) and acetonitrile (95%) in isocratic mode at a flow rate of 0.8 mL/min. The column temperature was set to 30°C and the detection wavelength was 290 nm. The elution time of α-tocopherol was 7.6 min.

The theoretical encapsulation efficiency (%EE) was determined as the ratio between the measured concentration and the theoretical concentration of α-tocopherol in the microcapsules:

$$\%EE = \frac{[Tocopherol]_{experimental}}{[Tocopherol]_{theoretical}} \times 100$$

The encapsulation efficiency corresponded to α-tocopherol encapsulated within the microcapsule and the free compound presents on the surface.

2.12. *In vitro* release kinetics assay in simulated gastrointestinal media

α-tocopherol release profile was assessed *in vitro* in simulated digestive media that artificially mimicked the pH and temperature conditions of the digestive transit. Two media were prepared: the simulated gastric digestion medium (acidic medium) and the simulated enteric digestion medium (neutral medium).

For the simulated gastric digestion medium, 90 mg of microcapsules were suspended in 4.5 mL of a buffer solution at pH 2.0 prepared to obtain a suspension of microcapsules at 20 g/L. For the preparation of 1L of buffer solution at pH 2.0 in a volumetric flask, 2 g of sodium chloride and 7 mL of HCl 37% were added to ultrapure water. The pH was then adjusted to 2.0 by adding 1M HCl or 1M sodium hydroxide (NaOH). The solution was adjusted with ultrapure water up to the mark. To test the effect of the proteolytic activity under gastric digestion conditions, 3.2 g/L of pepsin were added to the solution.

For the simulated enteric digestion medium, 90 mg of microcapsules were suspended in 4.5 mL of a buffer solution at pH 6.8 prepared to obtain a suspension of microcapsules at 20 g/L. For the preparation of 1L of buffer solution at pH 6.8 in a volumetric flask, 6.8 g of monobasic potassium phosphate (KH2PO4) and 77 mL of 0.2M NaOH were added to ultrapure water. The pH was adjusted to 6.8 by adding 1M NaOH or 1M HCl. The solution was adjusted with ultrapure water up to the mark. To test the effect of the proteolytic activity under intestinal digestion conditions, 10.0 g/L of pancreatin were added to the solution.

The microcapsule/buffer solution mixture was incubated in an oven at 37.5°C with orbital shaking at 180 rpm for a given time. The procedure was repeated for each sampling/analysis timepoint (t= 15, 30, 45, 60 and 90 minutes). The *in vitro* release experiments were performed in triplicate.

A liquid/liquid extraction in the presence of chloroform was needed to measure α-tocopherol released in the aqueous medium. This process used the following protocol: 4.5 mL of chloroform were added to the microcapsule suspension solutions. The mixture was shaken manually for 10s and left to phase shift (rapid phase shift <1 min). 1 mL of the chloroform phase was collected and centrifuged for 10 min at 12,000 rpm. The supernatant was diluted 1:1 with acetonitrile (v/v) and stored in a sealed vial for further HPLC analysis.

To assess the mechanism of α-tocopherol release, kinetic profile data were fitted with the following mathematical models: zero order, first order, Higuchi and Korsmeyer-Peppas models.

Zero order: $Q = Q_0 - K_0 t$

First order: $\log C = \log C_0 - {}^{K_1 t}/_{2.303}$

Higuchi: $Q = K_H t^{1/2}$ (Higuchi, 1963)

Korsmeyer-Peppas: ${}^{M_t}/_{M_\infty} = K_{KP} t^n$ (Korsmeyer et al., 1983)

Where Q is the cumulative amount of drug released at time t, Q_0 is the initial amount of drug (t=0); C is the concentration of drug in solution at time t, C_0 is the initial concentration of drug in solution; M_t/M_∞ is the fraction of drug released at time t, n is the diffusion exponent indicative of the transport mechanism; K_0, K_1, K_H and K_{KP} are the release rate constants for zero order, first order, Higuchi and Korsmeyer-Peppas kinetic models, respectively (Estevinho et al., 2013).

The correlation coefficient r^2 was used to compare the model applicability.

2.13. Statistical analysis

All measurements were carried out at least in triplicate using freshly prepared samples and data were reported as mean and standard deviation. The results were analyzed by one-way ANOVA, followed by a student's t-test to determine significant differences ($p < 0.05$) between experimental and control (PPI alone) samples. Graphs and data processing for mathematical models were constructed by Graph Pad Prism® 7 software (H.J. Motulsky, Prism 7 Statistics Guide, GraphPad Software Inc., San Diego, CA, USA).

3. Results and discussion

3.1. Effect of complex coacervation on the size distribution of emulsion droplets

Figure 1A shows the evolution of droplet size of emulsions formulated with PPI before and after homogenization at 250 bars. The results showed that the pre-emulsion formed with ultraturrax allowed forming an emulsion with a bimodal population with a mean droplet diameter of 35.8 µm. Homogenization at 250 bars allowed preparing an emulsion with a mean droplet diameter of 5.75 µm. Two droplet size populations were observed: a first submicron population accounting for 60% of the total population and a second population centered at 10 µm. The second population was related to a PPI fraction with poor solubility, due to the exposure of hydrophobic amino acid residues, making particle sub-structures difficult to disintegrate (Tsumura et al., 2005). When the distribution of the two particle size populations was compared, it appeared that homogenization allowed obtaining a finer emulsion likely to be more stable (Juttulapa et al., 2017). As an emulsion passes through the valve of the homogenizer, it is subjected to a combination of shear, cavitation forces and turbulent flow conditions, which disrupt the large droplets into smaller ones. Homogenization at 250 bars was therefore a key step in stabilizing the emulsion during the process. The second population centered at 10µm might be reduced by increasing the homogenization pressure. Same studies on pea proteins – oil emulsions at 400 bars homogenization explained that mechanical forces exerted on protein chains during high-pressure homogenization may cause an increase of their flexibilities. At the oil/water interface, proteins were able to unfold and exposed their hydrophobic regions at the interface and stabilize the emulsion by coating the interface (Le Priol et al., 2019).

A particle size analysis in liquid dispersions was performed during the different steps of the complex coacervation process of the four studied mixtures: PPI-TRAG, PPI-GAC and PPI-TARA. Only the results obtained at a protein/polysaccharide ratio of 10:1 (m/m) were presented (**Figure 1A, C, E**). The results corresponded to the particle size distribution during the following steps: homogenization of the PPI-oil solution at 250 bars, PPI-polysaccharide mixture and pH adjustment leading to complex coacervation. The curve corresponding to the emulsion by high-pressure homogenization was presented previously. An analysis of the polysaccharide alone in solution was also performed. **Table 1 supplemental data** describes the size of the different populations observed for each size distribution and the proportion of each population.

Regarding the PPI-GAC mixture, a slight increase in the volume of the second population (centered at 10 µm) was observed after addition of the polysaccharide. Therefore, it appeared that the addition of

gum arabic did not alter emulsion quality (**Figure 1C, Table 1 supplemental data**). According to our previous study of complex coacervation between PPI and GAC, no complex coacervate formed at pH 6.8 since the two biopolymers showed a negatively charge density (Carpentier et al., 2021). It can be assumed that polysaccharide was not absorbed to the droplet surfaces because of electrostatic repulsion between the negatively charged droplets and negatively charged polysaccharides, explaining the non-alteration of the emulsion quality (Gharsallaoui et al., 2010). However, after acidification of the medium to the optimal pH for the formation of complex coacervates from the PPI-GAC mixture, a significant change in particle size distribution was observed with a mean particle diameter of 13.1 µm compared to 5.75 µm for the PPI-oil emulsion while the submicron population (0.6 µm) observed in the PPI-oil emulsion disappeared after pH lowering. This increase of the droplet size was explained by the fact that GAC could adsorb to the surface of more than one emulsion droplet by electrostatic interactions between negatively charged GAC and positively charged PPI, acting as a polymeric link that promotes bridging flocculation (Gharsallaoui et al., 2010; Guzey & McClements, 2006). Also, this may be explained by the deposition of the coacervate, which binds together several oil droplets and encapsulates them within the same microcapsules. This phenomenon yields to polynucleated entities (Bordón et al., 2021). This bridging flocculation after complex coacervation can be attributed to formation electrostatic bonds and hydrogen bonds in the complex, which is consistent with FTIR results (Naderi et al., 2020). Lowering the pH seemed to increase the particle size through the formation of complex coacervates. An aggregation of the particles during mixing could explain the change in particle size. Wei *et al.* have investigated PPI stabilization in the presence of different polysaccharides and shown that lowering the pH of the protein from 7 to 3.5 increased the particle size due to protein flocculation (Wei et al., 2020). Since PPI possess both $-NH_3^+$ and $-COO^-$ groups, complex coacervates suspensions involved electrostatic interactions during complex coacervation formation but also PPI self-aggregation and counter-ion exchange.

Regarding tragacanth gum, a destabilization of the emulsion was observed after adding the tragacanth gum solution to the emulsion (**Figure 1A, Table 1 supplemental data**). The particle size distribution was heterogeneous with the presence of 5 different populations of particles, including a population with a size <1 µm corresponding to the emulsion. This difference in particle size distribution could be due to the particle size distribution of the added tragacanth gum solution. Indeed, the analysis of the particle size distribution of a dispersion containing 2% of tragacanth gum revealed particles with a size of about 129 µm. Farzi *et al.* have shown that in a dispersion containing 0.5% of tragacanth gum, particles also had a polydisperse distribution and a D(4.3) of 130 µm for gums from three different species (Farzi et al., 2015). This polydisperse system was due to the presence of two different polysaccharides: tragacanthin and bassorin. Tragacanthin is a branched polymer that is highly soluble in water, while bassorin is considered as an insoluble polysaccharide capable of forming aggregates in solution (López-Franco et al., 2009). Here, the population with a size of 100 µm seemed to correspond to the insoluble fraction of tragacanth gum (bassorin) and the population with a size >100 µm to the soluble fraction (tragacanthin). After pH adjustment, the size distribution was less polydisperse than before pH adjustment. Three populations were obtained: a population (accounting for 47% of the fraction) with a size of 120 µm and a population (accounting for 35% of the fraction) with a size of 4.4 µm, corresponding to the formation of complex coacervates between tragacanth gum and PPI. The last population (accounting for 18% of the fraction) corresponded to the unreacted PPI-oil emulsion. The submicron fraction corresponding to the emulsion was no longer present after pH adjustment and this could be due to the formation of aggregates after complex coacervation.

Finally, the addition of tara gum to the PPI-oil emulsion resulted in the formation of particles with a polydisperse distribution, as with the first two polysaccharides (**Figure 1E, Table 1 supplemental data**). The presence of an insoluble fraction in tara gum could explain the presence of the population

with a size of 57 µm. The analysis of the distribution of tara gum alone in solution confirmed this hypothesis with the presence of a population with a size of 130 µm. After pH adjustment, the emulsion appeared less destabilized. This could be explained by the fact that tara gum is a non-ionic galactomannan and therefore did not form complex coacervates with PPI. Therefore, pH adjustment only led to protein self-aggregation. This was further confirmed by the fact that the pH of the solution was adjusted to the optimal pH at 4.5, corresponding to the isoelectric point of the protein. The study of the association between PPI and a galactomannan from konjac gum by Wei *et al.* has shown similar results. According to the authors, the small change in particle size could be due to the fact that the galactomannan was neutral and therefore did not aggregate with the protein (Wei et al., 2020).

When comparing the size distribution of the suspensions after pH adjustment in the presence of gum arabic or tragacanth gum, a monomodal population was obtained in the presence of gum arabic while in the presence of tragacanth gum, a bimodal distribution was observed. Thus, gum arabic could reduce the alteration of the emulsion quality compared to tragacanth gum.

We also investigated the change in size distribution of suspended particles depending on the polysaccharide (tragacanth gum, gum arabic or tara gum) and the protein/polysaccharide ratio (1:1, 2:1, 5:1 and 10:1) (m/m) used (**Figure 1B, D, F**). **Table 2 supplemental data** shows the size of the different populations observed for each particle size distribution and the percentage of each population. The different solutions were analyzed after pH adjustment, inducing the complex coacervation process.

When gum arabic was used, the distribution of suspended particles was monomodal regardless of the ratio used (**Figure 1D**). Apart from the 1:1 ratio, the suspension size decreased with the decrease in gum arabic proportion (the size of the major peak decreased from 34.8 µm at the 2:1 ratio to 13.1 µm at the 10:1 ratio) (**Table 2 supplemental data**). It could be assumed that the presence of PPI stabilized the emulsion under high pressure homogenization more than increasing the polysaccharide load. Also, the increase of polysaccharide proportion in the mixture lead to an increase of bridging flocculation between oil droplets by interacting with positively charged proteins – oil droplets.

When tragacanth gum was used, a bimodal distribution was found regardless of the ratio used (**Figure 1B**). The size of the main particle population ranged between 40 and 200 µm. The size of the second population ranged between 1 and 20 µm. As for gum arabic, the diameter of the major peak decreased with the decrease in polysaccharide proportion in the mixture with a similar mechanism (**Table 2 supplemental data**).

The same observation was made for tara gum (**Figure 1F**). Thus, it was assumed that the presence of the polysaccharide affected the emulsion quality by increasing particle size distribution.

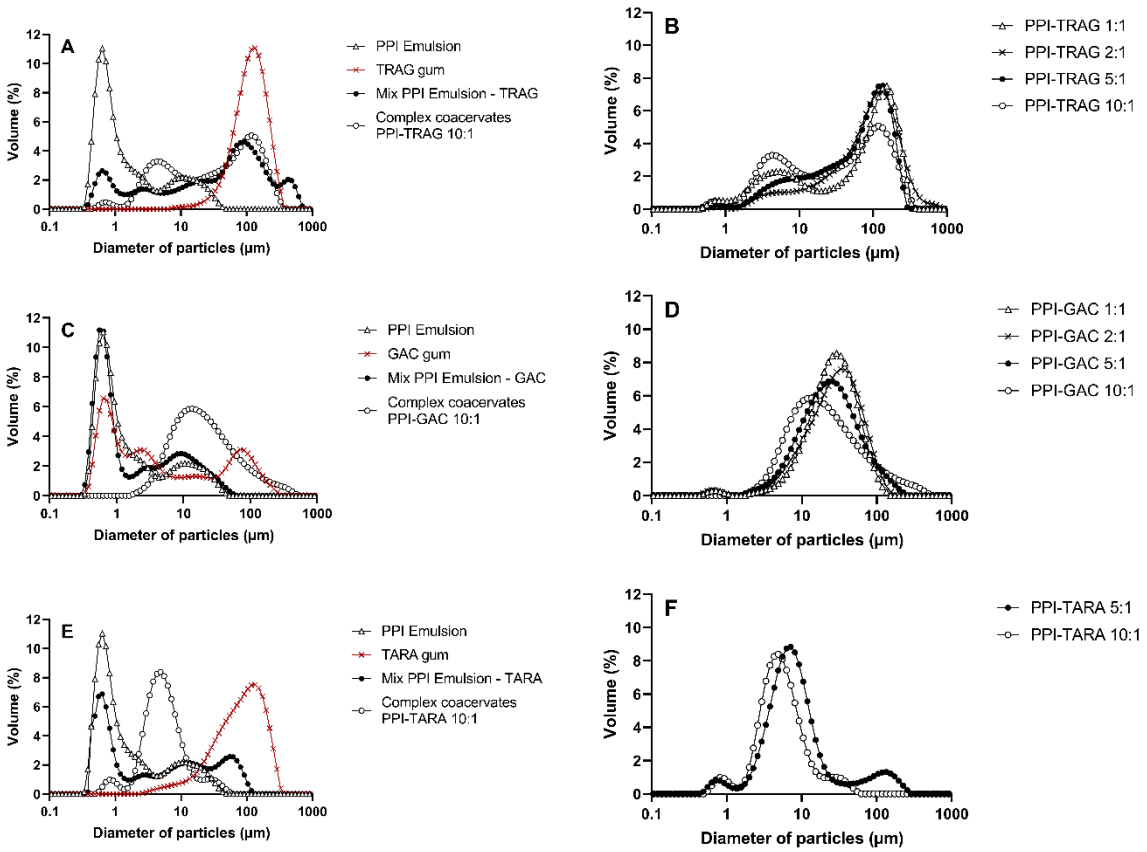

Figure 1: Evolution of droplet/particle size distribution in dispersions during the complex coacervation process for: PPI-TRAG (A), PPI-GAC (C) and PPI-TARA (E), all at the 10:1 ratio. -x- corresponds to the polysaccharide solution alone; -Δ- corresponds to the PPI-oil emulsion after homogenization at 250 bars; -●- corresponds to the PPI-polysaccharide mixture before pH adjustment; -○- corresponds to the PPI-polysaccharide mixture after pH adjustment. Effect of the protein/polysaccharide ratio on the particle size distribution of PPI-TRAG (B), PPI-GAC (D) and PPI-TARA (F) encapsulating α-tocopherol.

3.2. Characteristics of microcapsules

The influence of the polysaccharide and protein/polysaccharide ratio used on different parameters such as the moisture content, mean particle diameter, atomization efficiency and encapsulation efficiency were studied (**Table 2**).

Moisture content is a key parameter, which is related to the drying efficiency. A lower moisture contents limits the ability of water to act as a plasticizer and to reduce the glass transition temperature (Ferrari et al., 2012). The moisture content obtained for atomized powders was of 3-4%. The values obtained for the different protein/polysaccharide mixtures were similar to the moisture content of microcapsules containing only PPI. The nature of the polysaccharide associated with PPI or the PPI/polysaccharide ratio did not significantly influence the moisture content of the spray-dried powders. The nature of the polysaccharide associated with PPI or the PPI/polysaccharide ratio did not seem to significantly influence the moisture content of the spray-dried powders. According to Botrel *et al.*, the moisture content of spray-dried particles was mainly influenced by the variables of the drying process such as the process inlet air temperature (Botrel et al., 2014). Changes in the composition of the encapsulating wall had little effect on the moisture content of the powder.

The analysis of spray-dried particle size revealed micrometer-scale particles with a diameter D(V; 0.5) ranging between 10 and 80 µm in the different mixtures. Drying a PPI emulsion encapsulating a hydrophobic active ingredient enabled the formation of microparticles with the smallest size (10.6 µm). The results were in accordance with the results usually found in the literature (Costa et al., 2015; Pereira et al., 2009). In the presence of gum arabic, the microparticle size did not significantly vary depending on the protein/polysaccharide ratio. In the presence of tragacanth gum, the mean diameter decreased with the increase in protein/polysaccharide ratio (mean particle size ranging between 78.3 and 24.4 µm for the 1:1 and 10:1 PPI-TRAG ratios, respectively). This could be explained by the increase in viscosity with increasing polysaccharide proportion. Xie *et al.* have shown that decreasing the viscosity of spray-dried preparations reduced microparticle size (Xie et al., 2010). In the presence of tara gum, a small decrease in particle size was observed with the increase in protein/polysaccharide ratio. This could also be due to the viscosity of the solutions. In the presence of Tara gum, particle size significantly increased compared to PPI alone, attributed to the viscosity of the solutions.

The encapsulation efficiency (%EE) of the microcapsules was affected by the ability of the encapsulating material to form a continuous layer around the oil drops, reducing coalescence phenomena (Bajaj et al., 2017). The encapsulation efficiencies of microcapsules with a theoretical load of 25% of hydrophobic active ingredient are presented in **Table 2**. PPI encapsulation efficiency was of 53.4%. Different trends were observed depending on the nature of the polysaccharide. For the PPI-GAC interaction, a significant increase in encapsulation efficiency was observed with a decrease in protein/polysaccharide ratio (77.4% at the 1:1 PPI-GAC ratio *versus* 42.7% at the 10:1 ratio). The addition of carbohydrate to the proteinaceous wall system reduces the diffusion of the solvent through the matrix, due to the formation of a dry crust and a continuous glass phase in which proteins are dispersed, increasing the microencapsulation efficiency (Costa et al., 2015; Rosenberg et al., 1990). This phenomenon was not observed in the case of other protein-polysaccharide interactions. For tragacanth gum and tara gum, no trend was observed with the various ratios.

The atomization efficiency (%SY) of the microcapsules, presented in **Table 2**, varied from 53 to 85% depending on the mixture. No trend with the spray efficiency was observed between the different ratios of the same mixture. The spray efficiencies obtained could be related to the presence of powders adhering to the spray-dryer during the process or to the loss of fine particles through the spray tower filters. For tragacanth gum and tara gum, the atomization yields were lower. For tara gum, the yield did not exceed 53%. According to Nesterenko *et al.*, this decrease in spray yield could be related to the viscosity of emulsions (Nesterenko et al., 2012). High viscosities interfere with the atomization process and lead to the formation of elongated and large droplets that adversely affect the drying rate (Rosenberg et al., 1990).

Table 2: Characteristics of the prepared α-tocopherol microcapsules. Statistical significance was assessed by the one-way ANOVA test (n=3). The statistical differences between values obtained with mixture samples and negative control (PPI alone) are indicated by the letters a ($p < 0.05$), b ($p < 0.01$), c ($p < 0.001$) and d ($p < 0.0001$).

Matrix	Ratio	Encapsulation efficiency (%)	Moisture content (%)	Particle size D (V ;0,5) (µm)	Spray-drying yield (%)
PPI	-	53.4 ± 3.4	3.6 ± 0.1	11.5 ± 1.3	86
PPI-GAC	1:1	77.4 ± 0.9 ^{d}	3.2 ± 0.3	15.5 ± 0.7	85

	2:1	54.1 ± 2.9	3.9 ± 0.2	15.2 ± 0.3	59
	5 :1	44.6 ± 3.7	3.4 ± 0.1	15.6 ± 1.3	77
	10:1	42.7 ± 1.0 [a]	3.2 ± 0.4	16.6 ± 0.3	57
PPI-TRAG	1:1	54.1 ± 7.3	4.2 ± 0.4	78.3 ± 6.7 [d]	71
	2:1	71.2 ± 4.5 [b]	3.3 ± 0.1	57.5 ± 4.6 [c]	59
	5:1	52.1 ± 2.7	4.2 ± 0.2	14.6 ± 5.6	43
	10:1	61.2 ± 1.9	3.3 ± 0.0	24.4 ± 1.8	55
PPI-TARA	5:1	48.8 ± 1.1	3.8 ± 0.1	75.9 ± 18.4 [d]	53
	10:1	63.1 ± 2.7	3.5 ± 0.3	51.7 ± 23.1 [b]	53

3.3. Morphological properties of the microcapsules

The microcapsule surface of the PPI-TRAG, PPI-GAC and PPI-TARA microcapsules at the 5:1 ratio and PPI microcapsules was analyzed (**Figure 2**).

The SEM observations showed particles with a size of about 10 μm. The microcapsules presented a deflated spherical shape characteristic of the spray drying process, in which material shrinkage occurs due to the rapid water loss during the initial stages of drying (Francisco et al., 2020). Overall, the topography of the surface of PPI particles encapsulating α-tocopherol showed a smooth surface and the absence of cracks or pores, protecting α-tocopherol. According to Oliveira *et al*., the external surface of particles without cracks or breaks promotes low gas permeability, higher retention and protection of active ingredients (Oliveira et al., 2007). Spray-dried microcapsules are essentially spherical but morphological changes may be observed depending on the nature of the carrier used (Walton & Mumford, 1999). Especially, Microparticles with rough and/or invaginated surfaces present accelerated release of encapsulated material due to a greater surface area (Walton & Mumford, 1999). At the highest magnification, the absence of pores was evident, but small concavities were present, making the particle surface look like a "wrinkled" surface. In the study of the encapsulation of tuna oil by complex coacervates between milk proteins and gum arabic, the concavities were mainly related to the presence of the proteins within the wall of the spray-dried particles (Eratte et al., 2015).

The analysis of the surface of the PPI-TRAG microcapsules showed a smooth, pore-free surface as described in the initial analyzes. For PPI-GAC microcapsules, the surface was also smooth but cavities were present. At the lowest magnification, these cavities looked like pores. However, an analysis at the highest magnification confirmed the absence of pores and the presence of cavities. These cavities could be related to the second phase of spray drying, leading to a deformation of the encapsulating wall. Finally, for PPI-TARA microparticles, the morphology appeared to be intermediate between the smooth surface of the PPI-TRAG particles and the rough surface observed for microparticles of PPI

alone. This intermediate structure was related to the presence of tara gum, that facilitated particle smoothing due to the plasticizing properties of the polysaccharide. This phenomenon has been previously reported, in particular with maltodextrin (Jun-xia et al., 2011).

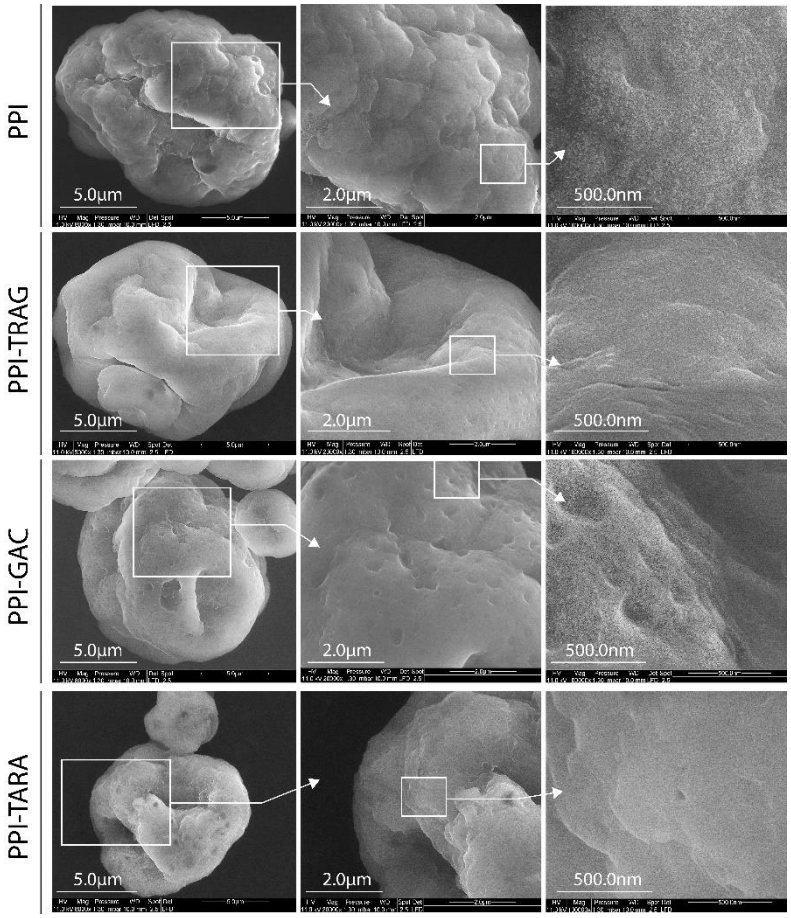

Figure 2: SEM observations of the different formulations of PPI, PPI-GAC, PPI-TRAG and PPI-TARA microcapsules at the 5:1 ratio at x8,000, x20,000 and x100,000 magnifications.

3.4. FTIR analysis

Figure 3 shows the FTIR spectra of spray-dried PPI-TRAG microcapsules at the 2:1 ratio compared to FTIR spectra of the biopolymers forming the coating material (PPI and TRAG alone) and the hydrophobic mixture. The other microcapsules presented a similar behavior.

The FTIR spectra of PPI and TRAG were characterized in our previous work (Carpentier,2021). The study showed that the complex coacervate of PPI-TRAG led to a shift of the peaks of amide I, II and III of pea proteins from 1631, 1523 and 1390 cm^{-1} in PPI to 1628, 1520 and 1377 cm^{-1} in PPI-TRAG. This shift was attributed to the association of negatively charged TRAG with positively charged PPI during complex coacervates formation.

The spectrum of the mixture of sunflower oil and α-tocopherol (SOT) showed a small peak at 3,008 cm^{-1} associated with the stretching of cis double-bond (=CH). Peaks at 2,923 and 2,854 cm^{-1} were respectively due to asymmetric and symmetric stretching vibrations of the aliphatic $-CH_2$ and $-CH_3$ groups. The peak at 1,744 was known as absorption bands of triglycerides (C=O of triglycerides or esters). The peak at 1,460 cm^{-1} was associated with C=C stretching in the phenyl skeletal and methyl asymmetric bending of α-tocopherol and bending vibrations of the $-CH_2$ and $-CH_3$ groups of sunflower oil. The peak at 1,377 cm^{-1} was associated with rocking vibrations of CH bonds of cis-

disubstituted olefins and methyl symmetric bending of α-tocopherol. The peak at 1,091 cm^{-1} was associated with stretching vibrations of the C-O ester group. The peak at 722 cm^{-1} corresponded to rocking vibrations of methylene (-CH_2) and out of plan vibrations of cis-disubstituted olefins (Che Man et al., 2005; Ma et al., 2021; Ozulku et al., 2017; Sim & Ting, 2012; Vlachos et al., 2006).

The FTIR spectra of PPI, TRAG, the hydrophobic mixtures and the PPI-TRAG microcapsules at the 2:1 ratio showed that the functional groups present in the microcapsules were similar to functional groups of PPI and tragacanth gum.

The PPI structure clearly dominated in the spectrum of PPI-TRAG complexes due to the higher protein ratio (2:1), but it was different from that of each individual biopolymer. The spectrum of PPI-TRAG microcapsules at the 2:1 ratio showed all the characteristic peaks of the α-tocopherol/sunflower oil mixture, indicating that the active compound was incorporated into the microcapsules. FTIR measurements did not allow to distinguish the α-tocopherol encapsulated into the microcapsules from the free α-tocopherol present on the surface.

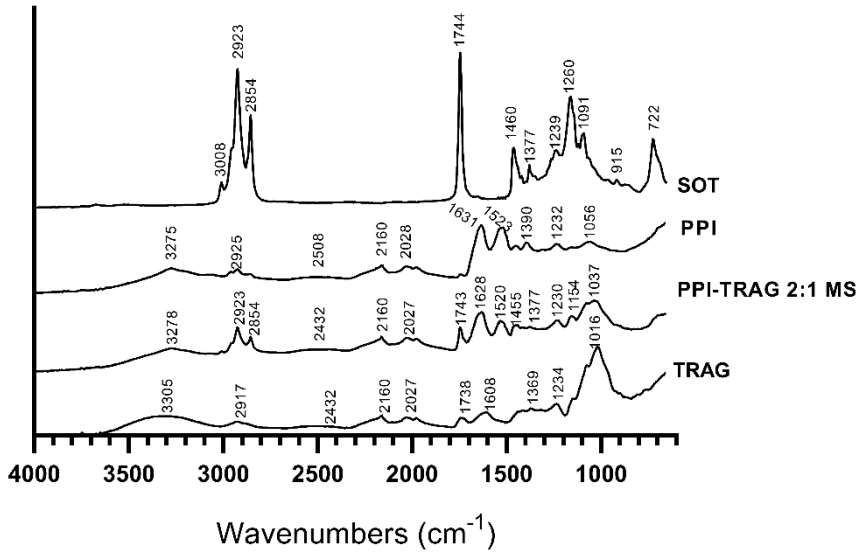

Figure 3: FTIR spectra of the PPI-TRAG microcapsules prepared at the 2:1 ratio compared to the spectra of PPI, TRAG and SOT (sunflower oil/α-tocopherol mixture at a 90:10 ratio) alone.

3.5. Influence of the pH on the microcapsule release behavior

Figure 4 shows the release profiles of α-tocopherol in acidic medium (pH 2.0) (**Figure 4 A,C,E**) and in neutral medium (pH 6.8) (**Figure 4 B,D,F**) in the presence of PPI or the complex coacervates from the PPI-GAC , PPI-TRAG and PPI-TARA mixtures at different ratios (1:1, 2:1, 5:1 and 10:1). The percentage of α-tocopherol released was expressed relative to the theoretical α-tocopherol level in microcapsule formulations (25% m/m).

For PPI microcapsules alone, a similar release profile was observed regardless of the pH (6.8 or 2.0). At 90 minutes, the release was of 40% at pH 2.0 and 6.8. In both media, the release kinetics can be associated with a two-step biphasic process, with a first step of rapid release (or "burst effect") followed by a second step of lower release (Luo et al., 2011).

In the presence of gum arabic, different release profiles were obtained.

In acidic medium (pH 2.0), the release profile differed from that of PPI microcapsules alone (**Figure 4C).** The release of α-tocopherol increased with the increase in protein/polysaccharide ratio, from 15

to 54% for the 1:1 and 10:1 ratios, respectively, at 90 minutes. The 1:1 and 2:1 ratios were associated with a similar release profile <20% in the acidic medium. The burst effect observed until t=30 minutes was significantly reduced for both ratios compared to the 5:1 ratio. The addition of gum arabic to the mixture improved protection at an acidic pH. However, increasing the ratio (>5:1) increased the release of α-tocopherol, up to release levels greater than those obtained with PPI alone. In neutral medium (pH 6.8), an increased release of α-tocopherol was observed with an increase in protein/polysaccharide ratio, except for the 2:1 ratio (**Figure 4D**). The release profiles at the 5:1 and 10:1 ratios were close to the release profile of PPI alone. The 2:1 ratio was associated with the highest release (release of 39%). The comparison of the release profiles in the two media showed that the presence of gum arabic resulted in a partial protection (15-20%) in the acidic medium and in a release in the neutral medium for ratios <5:1. The difference in release profiles between the acidic and neutral media could be due to a pH-dependent fragility of the microcapsules. At pH 2.0, the electrostatic interactions between PPI and gum arabic were favorable, the biopolymers having opposite charges. On the other hand, in the neutral medium, the pH was higher than the isoelectric point of PPI and the system was dominated by the presence of repellent electrostatic interactions, due to the predominance of negative charges between the two biopolymers (Bastos et al., 2020). Therefore, the complexes were destabilized, resulting in a greater release of α-tocopherol. For a pH-dependent behavior adapted to the protection/release of a hydrophobic active ingredient in a monogastric system, the 2:1 PPI-GAC ratio appeared to be the most effective with a release <20% in acidic medium and a higher release in neutral medium (release of 40%). For higher ratios, the opposite phenomenon was observed with a higher release in acidic medium than in neutral medium (α-tocopherol release of 50% at pH 2.0 *versus* 33% at pH 6.8 after 120 minutes for the 5:1 ratio).

The release profiles of the PPI-TRAG mixture at the 1:1, 2:1, 5:1 and 10:1 ratios in acidic and neutral media are shown in **Figure 4A, B**. At acidic pH, the release of α-tocopherol increased with the protein/polysaccharide ratio (**Figure 4A).** As with gum arabic, the 1:1 and 2:1 ratios were associated with a low release at acidic pH (release <10%). For ratios >5:1, the release profile was similar to that of PPI alone with release of the active ingredient after 10 minutes. Thus, the presence of tragacanth gum improved protection in acidic environments. A comparison of the release profiles obtained at 120 minutes in the two media showed a different behavior according to the protein/polysaccharide ratio tested as demonstrated in PPI-GAC mixtures. As with gum arabic, α-tocopherol release increased at pH 6.8 with increasing protein/polysaccharide ratio, except for the 5:1 ratio (**Figure 4B**). At the 5:1 ratio, the release of α-tocopherol was greater than in the presence of PPI alone. For the 5:1 and 10:1 ratios, a biphasic release system similar to that of PPI alone was observed with a first step of rapid release observed until t=60 minutes and a second step of slow release thereafter. This phenomenon has been observed in a study describing the encapsulation of β-carotene by complex coacervates of caseinate and tragacanth gum (Jain et al., 2016). In this study, the rapid release effect was associated with a rapid release of the active ingredient adsorbed at the microcapsule surface or a loss of wall integrity during particle drying. The slower release was related to the mixed mechanisms of penetration, solubilization and diffusion of the lipophilic phase through the polymeric caseinate-gum tragacanth wall.

Figure 4 E, F shows the release profiles of the PPI-TARA mixture at the 5:1 and 10:1 ratios in acidic (pH 2.0) and neutral (pH 6.8) media. In the presence of tara gum, the release of α-tocopherol varied depending on the ratio. At pH 2.0, the release of α-tocopherol was lower in the presence of tara gum (**Figure 4E**). The higher the proportion of tara gum was, the more the mixture reduced the release of the active ingredient in an acidic environment. At pH 6.8, the release of α-tocopherol was greater with the 5:1 PPI-TARA ratio than with PPI alone (40% and 33%, respectively, after 90 minutes of

incubation) (**Figure 4F**). For the 10:1 ratio, the release was lower (25% after 90 minutes of incubation). The difference in stability between the 5:1 and 10:1 ratios could be due to the difference in emulsion particle size between the two formulations. The PPI-TARA mixture had a smaller mean emulsion droplet diameter at the 10:1 ratio than at the 5:1 ratio. This difference in emulsion size could improve the stability of PPI-TARA microcapsules at the 10:1 ratio at pH 6.8 and thus limit the release of the active ingredient. In a similar study, the development of emulsions from milk proteins and guar gum delayed the release of vitamins under simulated gastric conditions and led to a release in a simulated enteric environment associated with stronger effects than in the presence of gum arabic (Li et al., 2011). Guar gum has structural similarities with tara gum in terms of galactomannan composition, only the mannose/galactose ratio differs (Wu et al., 2017). However, the comparison of the two release profiles of the PPI-TARA mixture at pH 6.8 and 2.0 did not show any significant difference in active ingredient release profiles and no conclusion on the pH-dependent release properties of the microcapsules could be drawn for the PPI-TARA mixture.

Studying the influence of the loaded polysaccharide on the release of α-tocopherol at the 2:1 protein-polysaccharide ratio, gum arabic and tragacanth gum appeared to provide the best protection of the active ingredient in acidic medium since they were associated with the lowest release rate (<20% after two hours). Among these two gums, tragacanth gum showed an interesting gastroresistant potential because its associated release rate did not exceed 10%. At pH 6.8, the highest release of α-tocopherol was obtained with gum arabic with a release of the active ingredient of 39% after 90 minutes. Tragacanth gum was again associated with the lowest α-tocopherol release rate after 90 minutes (release of 21%).

These profiles highlighted the interesting potential of tragacanth gum associated with PPI for the protection of a lipophilic active ingredient in an acidic environment. Despite a lower release at pH 6.8 than with gum arabic, the complex coacervation between PPI and tragacanth gum could be an interesting alternative to gum arabic commonly used for the delivery of liposoluble active ingredients with a pH-dependent controlled release. These formulations were used in the release behavior studies performed under enzymatic digestion conditions described below.

In addition, a trend in the change in microparticle release properties was also observed depending on the nature of the polysaccharide and protein/polysaccharide ratio used. For gum arabic and tragacanth gum, in particular, the mixtures appeared to have similar behaviors depending on the ratio. A gastroprotective behavior was observed at the 1:1 and 2:1 ratios and an opposite behavior was observed when the ratio was increased (from the 5:1 ratio) with a higher release in acidic medium than in neutral medium.

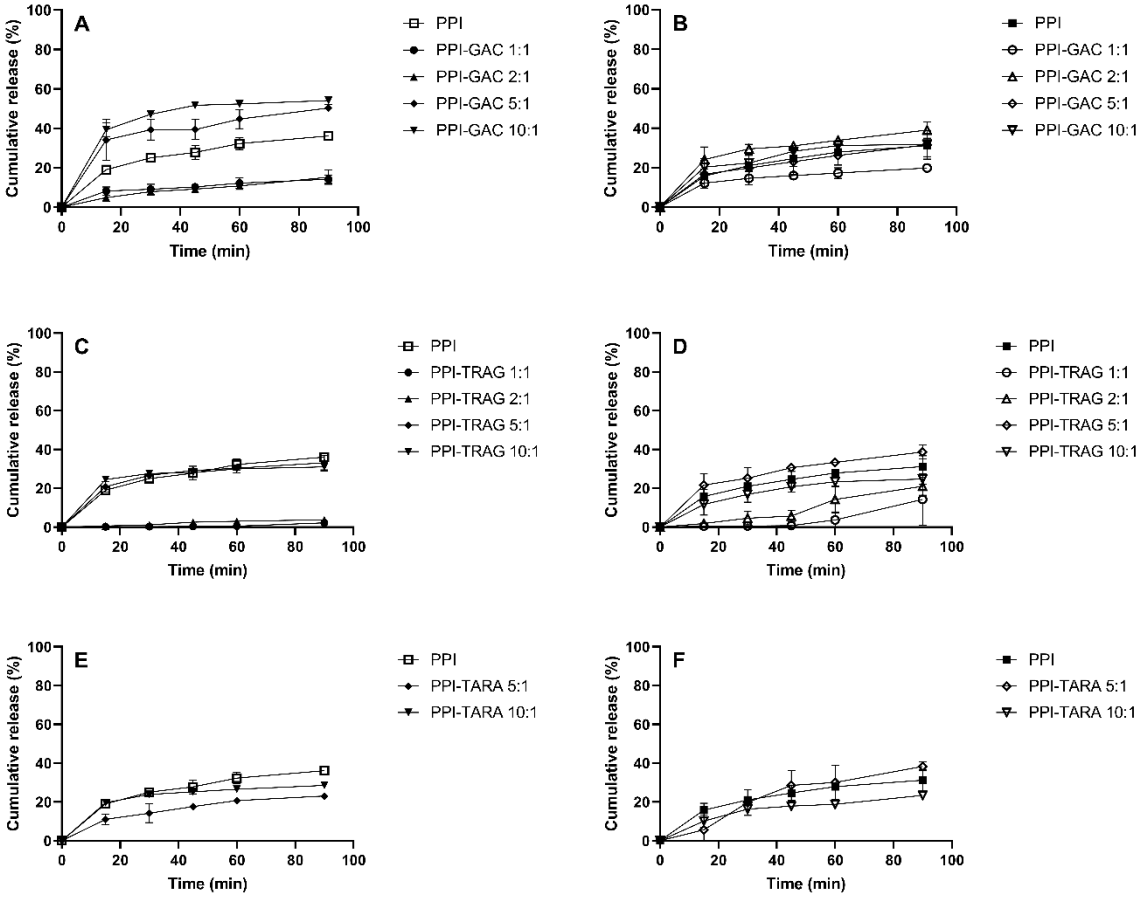

Figure 4: Influence of the protein/polysaccharide ratio in PPI-TRAG, PPI-GAC and PPI-TARA microcapsules on the time-dependent release profile of α-tocopherol at pH 2.0 (A, C, E) and pH 6.8 (B, D, F).

3.6. Influence of digestive enzymes on the microcapsule release behavior

α-tocopherol encapsulated in PPI alone and in complex coacervates between PPI and GAC and between PPI and TRAG at the 1:1 and 2:1 ratios was incubated at 37°C for 90 minutes under simulated gastric (pepsin solution at pH 2.0) or intestinal (pancreatin solution at pH 6.8) conditions to assess its release profile (**Figure 5**). These formulations were selected from the previous release studies for their gastroprotective properties and compared to the control formulation (PPI alone).

α-tocopherol release was increased when the digestive enzymes were added in the simulated gastric and intestinal media compared to the buffered solutions.

For the microcapsules of PPI alone, the change in α-tocopherol release was more rapid under gastric conditions than under intestinal conditions with a complete release of α-tocopherol (100%) achieved after 45 and 90 minutes, respectively (**Figure 5 A, B**). The PPI used to form these microcapsules consist of a heterogeneous mixture of proteins of varying molecular weight and complex assemblies of subunits linked together by disulfide bridges or low energy bonds. In the presence of pepsin, PPI were sensitive to hydrolysis, leading to the destabilization of their structure at acid pH (Perrot, 1995).

Associated with gum arabic, PPI showed equivalent gastroprotective properties at the 1:1 and 2:1 (m/m) ratios in buffer solutions at pH 2.0. However, the presence of proteolytic enzymes such as pepsin destabilized the microcapsules since α-tocopherol release varied from 16% in buffer solution to respectively 72% and 100% at the 1:1 and 2:1 ratios in pepsin solution after 90 minutes of

incubation. The release profile with PPI-GAC microcapsules at the 2:1 ratio was slightly faster compared to PPI alone, with a complete release of α-tocopherol after 30 minutes in pepsin solution. The gastroprotective properties increased with the increase in polysaccharide amount in the complex coacervate formulation. Under intestinal conditions, PPI-GAC microcapsules at the 2:1 ratio showed a profile similar to that of PPI alone. With PPI-GAC microcapsules at the 1:1 ratio, the release rate of α-tocopherol was lower, showing again the proteolytic resistance of microcapsules in the presence of polysaccharides. For PPI-GAC microcapsules, the pH-dependent behavior observed in aqueous media seemed to be lost in presence of proteolytic activity.

With the PPI-TRAG mixture, the gastroprotective properties were preserved under proteolytic conditions, especially for the PPI-TRAG mixture at the 1:1 ratio before 90 minutes. With the increase in PPI-TRAG ratio from 1:1 to 2:1, a decrease in gastroprotective properties was observed with an α-tocopherol release rate of 40% after 60 minutes. As with the PPI-GAC mixture, the gastroprotective properties increased with the increase in polysaccharide amount in the microcapsule matrix. Under intestinal conditions, the protective properties at both ratios were preserved in the presence of pancreatin since the release profiles were similar to those obtained in buffer solutions at pH 6.8. Compared to PPI-GAC, PPI-TRAG showed a better resistance to the proteolytic action of pancreatin and pepsin. An assumption could be made concerning the organization of the PPI-TRAG matrix compared to the PPI-GAC matrix. As the PPI-TRAG matrix was associated with a lower release in the presence of pepsin, it could be assumed that tragacanth gum was organized around PPI during the formation of complex coacervates, preventing PPI degradation by pepsin. For PPI-GAC, a less well-organized matrix between PPI and gum arabic could be assumed. This difference in organization between PPI and polysaccharides could be related to the solubility of the respective gum.

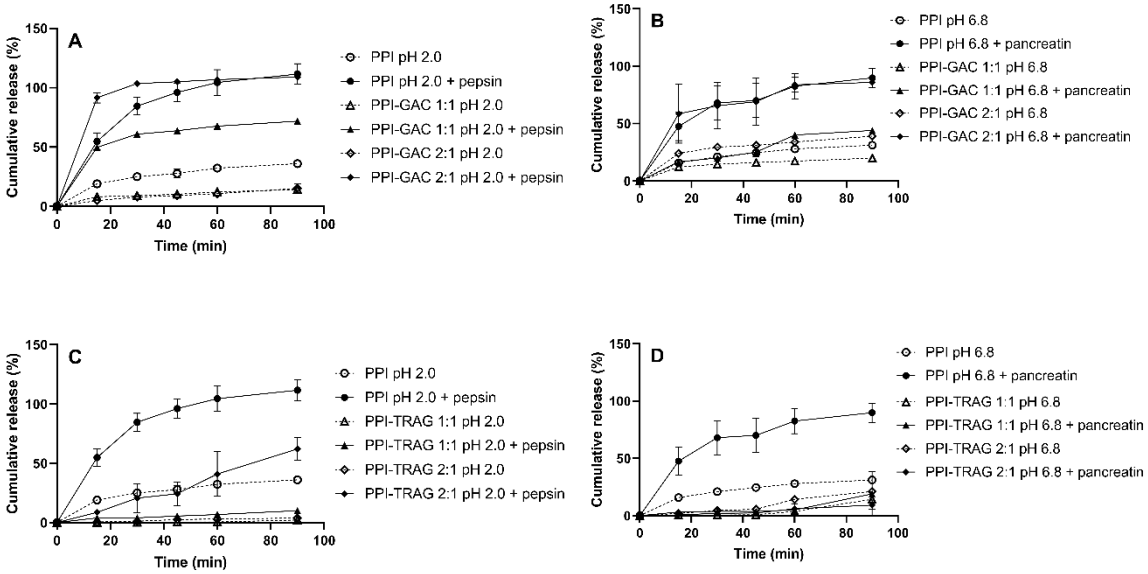

Figure 5: Influence of the protein/polysaccharide ratio in PPI-TRAG, PPI-GAC and PPI-TARA microcapsules on the time-dependent release profile of α-tocopherol in simulated digestive media at pH 2.0 (A, C) and pH 6.8 (B, D).

The release of an encapsulated active compound may be associated with different mechanisms, such as the disintegration or erosion of the polymeric skeleton, the diffusion through the wall and pores of the polymeric matrix or osmosis (Estevinho et al., 2013). The release profiles of α-tocopherol in

simulated digestive media were analyzed using different mathematical models: zero order, first order, Higuchi and Korsmeyer-Peppas model equations to identify the release mechanisms.

For PPI alone and PPI-GAC microcapsules, the equation that presented the best correlation coefficient r^2 with α-tocopherol release profile data was the Korsmeyer-Peppas model (**supplemental data Table 3**). The diffusion exponent n, used to interpret the main release mechanism, was determined from the model equation (**Table 3**). According to the literature, the transport is controlled by a Fickian diffusion (case I transport) when n is <0.43. When n ranges between 0.43 and 0.85, an anomalous transport associated with a non-Fickian diffusion occurs, resulting from a combination of diffusion mechanisms and swelling releases. When n is >0.85, the main transport mechanism is based on matrix swelling (n=0.85 case II transport; n >0.85 – super case transport) (Estevinho et al., 2013). For each release kinetics, the estimated n values were <0.43, indicating that α-tocopherol release was associated with a Fickian diffusion. This mechanism seemed to be in contradiction with the non-porous morphology of the microcapsules. A potential hypothesis may be formulated. As the association between protein and polysaccharide is governed by electrostatic interactions, the hydration of the capsule matrix in aqueous media destabilizes the electrostatic interactions between the protein and the polysaccharide, partially destructuring the wall of the microcapsule. This partial weakness of the wall could lead to the diffusion of α-tocopherol out of the microcapsule.

For PPI-TRAG microcapsules, the Korsmeyer-Peppas model equation also fitted with α-tocopherol release profile data. Surprisingly, the release mechanism was associated with super case II transport with n >0.85, except for PPI-TRAG at the 1:1 ratio under simulated gastric condition for which the release mechanism was associated with an anomalous transport. The release rate constant K_k was very low with these microcapsules, indicating the absence of a burst drug release (Obidike & Emeje, 2011) that suggested the resistance of microcapsules to proteolytic hydrolysis in the presence of tragacanth gum. The release rate constant and release exponent also suggested an erosion-controlled release mechanism for a 90-minute incubation time. It was observed in the first 60 minutes the linear and low release of α-tocopherol in both media leading to a n value superior to 0.85. It can be assumed, by pursuing the release profile at several hours, that the release of α-tocopherol from PPI-TRAG microcapsules will show a similar profile to PPI-GAC microcapsules. In this case, the release profile will be associated with Fickian diffusion.

Table 3: Parameters of the kinetic equations and corresponding correlation coefficients

		Korsmeyer Peppas		
		K_k	n	r^2
PPI	pH 2.0	24.04	0.3517	0.984
	pH 6.8	20.61	0.3311	0.991
PPI-GAC 1:1	pH 2.0	30.42	0.1939	0.998
	pH 6.8	2.52	0.6418	0.959
PPI-GAC 2:1	pH 2.0	73.58	0.09101	0.998
	pH 6.8	30.13	0.2347	0.990
PPI-TRAG 1:1	pH 2.0	0.45	0.6809	0.964
	pH 6.8	3.5E-4	2.416	0.917
PPI-TRAG 2:1	pH 2.0	0.40	1.121	0.989
	pH 6.8	0.01	1.486	0.969

4. Conclusion

The interactions between PPI and different polysaccharides were applied to the microencapsulation of α-tocopherol by spray drying of complex coacervates. The formulations, corresponding to different protein/polysaccharide mixtures, were characterized: PPI alone or associated with gum arabic, tragacanth gum or tara gum. The size distribution of emulsion oil droplets and complex coacervate particles in suspension showed an increase of the particles in suspension, correlated with electrostatic interactions between the negatively charged polysaccharide to the positively charged oil droplets. The comparison of the two charged polysaccharides showed that gum arabic allowed obtaining finer particles than tragacanth gum, due to the insoluble fraction of tragacanth gum. An influence of the protein/polysaccharide ratio was also shown as the increase of the polysaccharide proportion increased the size of the particles in suspension due to flocculation bridging by electrostatic interactions. In the presence of an uncharged polysaccharide (tara gum), no influence was observed on the particle size in the mixture, related to the absence of formation of complex coacervates. SEM observations of spray-dried microcapsule surface showed different properties depending on the polysaccharide used and the nature of the interaction between the plant proteins and the polysaccharides. α-tocopherol release in buffer media highlighted the pH-dependent behavior of gum arabic and tragacanth gum depending on the ratio used. An interesting acid stability was identified at the 1:1 and 2:1 protein/polysaccharide ratios in the case of PPI-GAC and PPI-TRAG due to electrostatic interactions between oppositely charged biopolymers. Among the two gums selected, tragacanth gum had the best acid stability. In the presence of proteolytic enzymes, the PPI-TRAG mixture maintained a stronger gastroprotective behavior compared to PPI-GAC matrices. Our results showed the ability of PPI to associate with plant polysaccharides, especially with tragacanth gum, to form an interesting pH-dependent coating for microencapsulation, resistant to gastric digestion and compatible with vegan/vegetarian applications.

Declaration of competing interest

The authors are not aware of any affiliations, memberships, funding or financial holdings that could affect the objectivity of this article.

Acknowledgements

We thank Dr. Egle Conforto from the CCA platform of La Rochelle University for her assistance in SEM observation. This work was financially supported by INNOV'IA and IDCAPS (La Rochelle, France).

5. References

Bajaj, P. R., Bhunia, K., Kleiner, L., Joyner (Melito), H. S., Smith, D., Ganjyal, G., & Sablani, S. S. (2017).

Improving functional properties of pea protein isolate for microencapsulation of flaxseed oil.

Journal of Microencapsulation, *34*(2), 218-230.

https://doi.org/10.1080/02652048.2017.1317045

728 Balaghi, S., Mohammadifar, M. A., & Zargaraan, A. (2010). Physicochemical and Rheological
729 Characterization of Gum Tragacanth Exudates from Six Species of Iranian Astragalus. *Food*
730 *Biophysics*, *5*(1), 59-71. https://doi.org/10.1007/s11483-009-9144-5
731 Barrow, C. J., Nolan, C., & Jin, Y. (2007). Stabilization of highly unsaturated fatty acids and delivery
732 into foods. *Lipid Technology*, *19*(5), 108-111. https://doi.org/10.1002/lite.200600037
733 Bastos, L. P. H., de Sá Costa, B., Siqueira, R. P., & Garcia-Rojas, E. E. (2020). Complex coacervates of β-
734 lactoglobulin/sodium alginate for the microencapsulation of black pepper (Piper nigrum L.)
735 essential oil : Simulated gastrointestinal conditions and modeling release kinetics.
736 *International Journal of Biological Macromolecules*, *160*, 861-870.
737 https://doi.org/10.1016/j.ijbiomac.2020.05.265
738 Bordón, M. G., Paredes, A. J., Camacho, N. M., Penci, M. C., González, A., Palma, S. D., Ribotta, P. D.,
739 & Martinez, M. L. (2021). Formulation, spray-drying and physicochemical characterization of
740 functional powders loaded with chia seed oil and prepared by complex coacervation. *Powder*
741 *Technology*, *391*, 479-493. https://doi.org/10.1016/j.powtec.2021.06.035
742 Botrel, D. A., de Barros Fernandes, R. V., Borges, S. V., & Yoshida, M. I. (2014). Influence of wall
743 matrix systems on the properties of spray-dried microparticles containing fish oil. *Food*
744 *Research International*, *62*, 344-352. https://doi.org/10.1016/j.foodres.2014.02.003
745 Carpentier, J., Conforto, E., Chaigneau, C., Vendeville, J.-E., & Maugard, T. (2021). Complex
746 coacervation of pea protein isolate and tragacanth gum : Comparative study with commercial
747 polysaccharides. *Innovative Food Science & Emerging Technologies*, *69*, 102641.
748 https://doi.org/10.1016/j.ifset.2021.102641
749 Che Man, Y. B., Ammawath, W., & Mirghani, M. E. S. (2005). Determining α-tocopherol in refined
750 bleached and deodorized palm olein by Fourier transform infrared spectroscopy. *Food*
751 *Chemistry*, *90*(1), 323-327. https://doi.org/10.1016/j.foodchem.2004.05.059

752 Chen, Y., Ye, R., & Liu, J. (2013). Understanding of dispersion and aggregation of suspensions of zein
753 nanoparticles in aqueous alcohol solutions after thermal treatment. *Industrial Crops and*
754 *Products*, *50*, 764-770. https://doi.org/10.1016/j.indcrop.2013.08.023
755 Chiu, Y. C., & Yang, W. L. (1992). Preparation of vitamin E microemulsion possessing high resistance
756 to oxidation in air. *Colloids and Surfaces*, *63*(3), 311-322. https://doi.org/10.1016/0166-
757 6622(92)80253-X
758 Chourpa, I., Ducel, V., Richard, J., Dubois, P., & Boury, F. (2006). Conformational Modifications of α
759 Gliadin and Globulin Proteins upon Complex Coacervates Formation with Gum Arabic as
760 Studied by Raman Microspectroscopy. *Biomacromolecules*, *7*(9), 2616-2623.
761 https://doi.org/10.1021/bm060131d
762 Conforto, E., Joguet, N., Buisson, P., Vendeville, J.-E., Chaigneau, C., & Maugard, T. (2015). An
763 optimized methodology to analyze biopolymer capsules by environmental scanning electron
764 microscopy. *Materials Science and Engineering: C*, *47*, 357-366.
765 https://doi.org/10.1016/j.msec.2014.11.054
766 Costa, A. M. M., Nunes, J. C., Lima, B. N. B., Pedrosa, C., Calado, V., Torres, A. G., & Pierucci, A. P. T. R.
767 (2015). Effective stabilization of CLA by microencapsulation in pea protein. *Food Chemistry*,
768 *168*, 157-166. https://doi.org/10.1016/j.foodchem.2014.07.016
769 Cuevas-Bernardino, J. C., Leyva-Gutierrez, F. M. A., Vernon-Carter, E. J., Lobato-Calleros, C., Román-
770 Guerrero, A., & Davidov-Pardo, G. (2018). Formation of biopolymer complexes composed of
771 pea protein and mesquite gum – Impact of quercetin addition on their physical and chemical
772 stability. *Food Hydrocolloids*, *77*, 736-745. https://doi.org/10.1016/j.foodhyd.2017.11.015
773 Devi, N., Hazarika, D., Deka, C., & Kakati, D. K. (2012). Study of Complex Coacervation of Gelatin A
774 and Sodium Alginate for Microencapsulation of Olive Oil. *Journal of Macromolecular Science,*
775 *Part A*, *49*(11), 936-945. https://doi.org/10.1080/10601325.2012.722854

776 Dong, Z., Ma, Y., Hayat, K., Jia, C., Xia, S., & Zhang, X. (2011). Morphology and release profile of
777 microcapsules encapsulating peppermint oil by complex coacervation. *Journal of Food*
778 *Engineering*, *104*(3), 455-460. https://doi.org/10.1016/j.jfoodeng.2011.01.011
779 Donsì, F., Senatore, B., Huang, Q., & Ferrari, G. (2010). Development of Novel Pea Protein-Based
780 Nanoemulsions for Delivery of Nutraceuticals. *Journal of Agricultural and Food Chemistry*,
781 *58*(19), 10653-10660. https://doi.org/10.1021/jf101804g
782 Ducel, V., Richard, J., Popineau, Y., & Boury, F. (2005). Rheological Interfacial Properties of Plant
783 Protein−Arabic Gum Coacervates at the Oil−Water Interface. *Biomacromolecules*, *6*(2),
784 790-796. https://doi.org/10.1021/bm0494601
785 Ducel, V., Richard, J., Saulnier, P., Popineau, Y., & Boury, F. (2004). Evidence and characterization of
786 complex coacervates containing plant proteins : Application to the microencapsulation of oil
787 droplets. *Colloids and Surfaces A: Physicochemical and Engineering Aspects*, *232*(2), 239-247.
788 https://doi.org/10.1016/j.colsurfa.2003.11.001
789 Duhoranimana, E., Yu, J., Mukeshimana, O., Habinshuti, I., Karangwa, E., Xu, X., Muhoza, B., Xia, S., &
790 Zhang, X. (2018). Thermodynamic characterization of Gelatin–Sodium carboxymethyl
791 cellulose complex coacervation encapsulating Conjugated Linoleic Acid (CLA). *Food*
792 *Hydrocolloids*, *80*, 149-159. https://doi.org/10.1016/j.foodhyd.2018.02.011
793 Eratte, D., McKnight, S., Gengenbach, T. R., Dowling, K., Barrow, C. J., & Adhikari, B. P. (2015). Co-
794 encapsulation and characterisation of omega-3 fatty acids and probiotic bacteria in whey
795 protein isolate–gum Arabic complex coacervates. *Journal of Functional Foods*, *19*, 882-892.
796 https://doi.org/10.1016/j.jff.2015.01.037
797 Eratte, D., Wang, B., Dowling, K., Barrow, Colin. J., & Adhikari, B. P. (2014). Complex coacervation
798 with whey protein isolate and gum arabic for the microencapsulation of omega-3 rich tuna
799 oil. *Food Funct.*, *5*(11), 2743-2750. https://doi.org/10.1039/C4FO00296B

Estevinho, B. N., Rocha, F., Santos, L., & Alves, A. (2013). Microencapsulation with chitosan by spray drying for industry applications – A review. *Trends in Food Science & Technology*, *31*(2), 138-155. https://doi.org/10.1016/j.tifs.2013.04.001

Farzi, M., Emam-Djomeh, Z., & Mohammadifar, M. A. (2013). A comparative study on the emulsifying properties of various species of gum tragacanth. *International Journal of Biological Macromolecules*, *57*, 76-82. https://doi.org/10.1016/j.ijbiomac.2013.03.008

Farzi, M., Yarmand, M. S., Safari, M., Emam-Djomeh, Z., & Mohammadifar, M. A. (2015). Gum tragacanth dispersions : Particle size and rheological properties affected by high-shear homogenization. *International Journal of Biological Macromolecules*, *79*, 433-439. https://doi.org/10.1016/j.ijbiomac.2015.04.037

Ferrari, C. C., Germer, S. P. M., Alvim, I. D., Vissotto, F. Z., & de Aguirre, J. M. (2012). Influence of carrier agents on the physicochemical properties of blackberry powder produced by spray drying : Spray drying of blackberry pulp. *International Journal of Food Science & Technology*, *47*(6), 1237-1245. https://doi.org/10.1111/j.1365-2621.2012.02964.x

Francisco, C. R. L., de Oliveira Júnior, F. D., Marin, G., Alvim, I. D., & Hubinger, M. D. (2020). Plant proteins at low concentrations as natural emulsifiers for an effective orange essential oil microencapsulation by spray drying. *Colloids and Surfaces A: Physicochemical and Engineering Aspects*, *607*, 125470. https://doi.org/10.1016/j.colsurfa.2020.125470

Gharsallaoui, A., Yamauchi, K., Chambin, O., Cases, E., & Saurel, R. (2010). Effect of high methoxyl pectin on pea protein in aqueous solution and at oil/water interface. *Carbohydrate Polymers*, *80*(3), 817-827. https://doi.org/10.1016/j.carbpol.2009.12.038

Ghayempour, S., Montazer, M., & Mahmoudi Rad, M. (2016). Encapsulation of Aloe Vera extract into natural Tragacanth Gum as a novel green wound healing product. *International Journal of Biological Macromolecules*, *93*, 344-349. https://doi.org/10.1016/j.ijbiomac.2016.08.076

824 Guzey, D., & McClements, D. J. (2006). Formation, stability and properties of multilayer emulsions for
825 application in the food industry. *Advances in Colloid and Interface Science*, *128-130*, 227-248.
826 https://doi.org/10.1016/j.cis.2006.11.021
827 Higuchi, T. (1963). Mechanism of sustained-action medication. Theoretical analysis of rate of release
828 of solid drugs dispersed in solid matrices. *Journal of Pharmaceutical Sciences*, *52*(12),
829 1145-1149. https://doi.org/10.1002/jps.2600521210
830 Jain, A., Thakur, D., Ghoshal, G., Katare, O. P., & Shivhare, U. S. (2016). Characterization of
831 microcapsulated β-carotene formed by complex coacervation using casein and gum
832 tragacanth. *International Journal of Biological Macromolecules*, *87*, 101-113.
833 https://doi.org/10.1016/j.ijbiomac.2016.01.117
834 Jun-xia, X., Hai-yan, Y., & Jian, Y. (2011). Microencapsulation of sweet orange oil by complex
835 coacervation with soybean protein isolate/gum Arabic. *Food Chemistry*, *125*(4), 1267-1272.
836 https://doi.org/10.1016/j.foodchem.2010.10.063
837 Juttulapa, M., Piriyaprasarth, S., Takeuchi, H., & Sriamornsak, P. (2017). Effect of high-pressure
838 homogenization on stability of emulsions containing zein and pectin. *Asian Journal of*
839 *Pharmaceutical Sciences*, *12*(1), 21-27. https://doi.org/10.1016/j.ajps.2016.09.004
840 Korsmeyer, R. W., Gurny, R., Doelker, E., Buri, P., & Peppas, N. A. (1983). Mechanisms of solute
841 release from porous hydrophilic polymers. *International Journal of Pharmaceutics*, *15*(1),
842 25-35. https://doi.org/10.1016/0378-5173(83)90064-9
843 Le Priol, L., Dagmey, A., Morandat, S., Saleh, K., El Kirat, K., & Nesterenko, A. (2019). Comparative
844 study of plant protein extracts as wall materials for the improvement of the oxidative
845 stability of sunflower oil by microencapsulation. *Food Hydrocolloids*, *95*, 105-115.
846 https://doi.org/10.1016/j.foodhyd.2019.04.026
847 Li, B., Jiang, Y., Liu, F., Chai, Z., Li, Y., & Leng, X. (2011). Study of the Encapsulation Efficiency and
848 Controlled Release Property of Whey Protein Isolate—Polysaccharide Complexes in

W1/O/W2 Double Emulsions. *International Journal of Food Engineering*, *7*(3). https://doi.org/10.2202/1556-3758.2321

Liu, S., Elmer, C., Low, N. H., & Nickerson, M. T. (2010). Effect of pH on the functional behaviour of pea protein isolate–gum Arabic complexes. *Food Research International*, *43*(2), 489-495. https://doi.org/10.1016/j.foodres.2009.07.022

López-Franco, Y., Higuera-Ciapara, I., Goycoolea, F. M., & Wang, W. (2009). Other exudates : Tragancanth, karaya, mesquite gum and larchwood arabinogalactan. In *Handbook of Hydrocolloids* (p. 495-534). Elsevier. https://doi.org/10.1533/9781845695873.495

Luo, Y., Zhang, B., Whent, M., Yu, L. (Lucy), & Wang, Q. (2011). Preparation and characterization of zein/chitosan complex for encapsulation of α-tocopherol, and its in vitro controlled release study. *Colloids and Surfaces B: Biointerfaces*, *85*(2), 145-152. https://doi.org/10.1016/j.colsurfb.2011.02.020

Ma, X., Liu, Y., Fan, L., & Yan, W. (2021). Ethyl cellulose particles loaded with α-tocopherol for inhibiting thermal oxidation of soybean oil. *Carbohydrate Polymers*, *252*, 117169. https://doi.org/10.1016/j.carbpol.2020.117169

Muhoza, B., Xia, S., Cai, J., Zhang, X., Duhoranimana, E., & Su, J. (2019). Gelatin and pectin complex coacervates as carriers for cinnamaldehyde : Effect of pectin esterification degree on coacervate formation, and enhanced thermal stability. *Food Hydrocolloids*, *87*, 712-722. https://doi.org/10.1016/j.foodhyd.2018.08.051

Naderi, B., Keramat, J., Nasirpour, A., & Aminifar, M. (2020). Complex coacervation between oak protein isolate and gum Arabic : Optimization & functional characterization. *International Journal of Food Properties*, *23*(1), 1854-1873. https://doi.org/10.1080/10942912.2020.1825484

Nazarzadeh Zare, E., Makvandi, P., & Tay, F. R. (2019). Recent progress in the industrial and biomedical applications of tragacanth gum : A review. *Carbohydrate Polymers*, *212*, 450-467. https://doi.org/10.1016/j.carbpol.2019.02.076

875 Nesterenko, A., Alric, I., Silvestre, F., & Durrieu, V. (2012). Influence of soy protein's structural
876 modifications on their microencapsulation properties : α-Tocopherol microparticle
877 preparation. *Food Research International*, *48*(2), 387-396.
878 https://doi.org/10.1016/j.foodres.2012.04.023
879 Nur, M., Ramchandran, L., & Vasiljevic, T. (2016). Tragacanth as an oral peptide and protein delivery
880 carrier : Characterization and mucoadhesion. *Carbohydrate Polymers*, *143*, 223-230.
881 https://doi.org/10.1016/j.carbpol.2016.01.074
882 Obidike, I. C., & Emeje, M. O. (2011). Microencapsulation enhances the anti-ulcerogenic properties of
883 Entada africana leaf extract. *Journal of Ethnopharmacology*, *137*(1), 553-561.
884 https://doi.org/10.1016/j.jep.2011.06.012
885 Oliveira, A. C., Moretti, T. S., Boschini, C., Baliero, J. C. C., Freitas, O., & Favaro-Trindade, C. S. (2007).
886 Stability of microencapsulated B. lactis (BI 01) and L. acidophilus (LAC 4) by complex
887 coacervation followed by spray drying. *Journal of Microencapsulation*, *24*(7), 685-693.
888 https://doi.org/10.1080/02652040701532908
889 Ozulku, G., Yildirim, R. M., Toker, O. S., Karasu, S., & Durak, M. Z. (2017). Rapid detection of
890 adulteration of cold pressed sesame oil adultered with hazelnut, canola, and sunflower oils
891 using ATR-FTIR spectroscopy combined with chemometric. *Food Control*, *82*, 212-216.
892 https://doi.org/10.1016/j.foodcont.2017.06.034
893 Pereira, H. V. R., Saraiva, K. P., Carvalho, L. M. J., Andrade, L. R., Pedrosa, C., & Pierucci, A. P. T. R.
894 (2009). Legumes seeds protein isolates in the production of ascorbic acid microparticles.
895 *Food Research International*, *42*(1), 115-121. https://doi.org/10.1016/j.foodres.2008.10.008
896 Perrot, C. (1995). Les protéines de pois : De leur fonction dans la graine à leur utilisation en
897 alimentation animale. *INRA Productions Animales, Paris: INRA*, *8*(3), 151-164.
898 Pryor, W. A. (2000). Vitamin E and heart disease : Basic science to clinical intervention trials. *Free*
899 *Radical Biology and Medicine*, *28*(1), 141-164. https://doi.org/10.1016/S0891-
900 5849(99)00224-5

Rosenberg, M., Kopelman, I. J., & Talmon, Y. (1990). Factors affecting retention in spray-drying microencapsulation of volatile materials. *Journal of Agricultural and Food Chemistry*, *38*(5), 1288-1294. https://doi.org/10.1021/jf00095a030

Roy, F., Boye, J. I., & Simpson, B. K. (2010). Bioactive proteins and peptides in pulse crops : Pea, chickpea and lentil. *Food Research International*, *43*(2), 432-442. https://doi.org/10.1016/j.foodres.2009.09.002

Sim, S. F., & Ting, W. (2012). An automated approach for analysis of Fourier Transform Infrared (FTIR) spectra of edible oils. *Talanta*, *88*, 537-543. https://doi.org/10.1016/j.talanta.2011.11.030

Sobel, R., Versic, R., & Gaonkar, A. G. (2014). Introduction to Microencapsulation and Controlled Delivery in Foods. In *Microencapsulation in the Food Industry* (p. 3-12). Elsevier. https://doi.org/10.1016/B978-0-12-404568-2.00001-7

Timilsena, Y. P., Adhikari, R., Barrow, C. J., & Adhikari, B. (2016). Microencapsulation of chia seed oil using chia seed protein isolate-chia seed gum complex coacervates. *International Journal of Biological Macromolecules*, *91*, 347-357. https://doi.org/10.1016/j.ijbiomac.2016.05.058

Timilsena, Y. P., Wang, B., Adhikari, R., & Adhikari, B. (2017). Advances in microencapsulation of polyunsaturated fatty acids (PUFAs)-rich plant oils using complex coacervation : A review. *Food Hydrocolloids*, *69*, 369-381. https://doi.org/10.1016/j.foodhyd.2017.03.007

Tsumura, K., Saito, T., Tsuge, K., Ashida, H., Kugimiya, W., & Inouye, K. (2005). Functional properties of soy protein hydrolysates obtained by selective proteolysis. *LWT - Food Science and Technology*, *38*(3), 255-261. https://doi.org/10.1016/j.lwt.2004.06.007

Vlachos, N., Skopelitis, Y., Psaroudaki, M., Konstantinidou, V., Chatzilazarou, A., & Tegou, E. (2006). Applications of Fourier transform-infrared spectroscopy to edible oils. *Analytica Chimica Acta*, *573-574*, 459-465. https://doi.org/10.1016/j.aca.2006.05.034

Walton, D. E., & Mumford, C. J. (1999). The Morphology of Spray-Dried Particles. *Chemical Engineering Research and Design*, *77*(5), 442-460. https://doi.org/10.1205/026387699526296

927 Wei, Y., Cai, Z., Wu, M., Guo, Y., Tao, R., Li, R., Wang, P., Ma, A., & Zhang, H. (2020). Comparative
928 studies on the stabilization of pea protein dispersions by using various polysaccharides. *Food*
929 *Hydrocolloids*, *98*, 105233. https://doi.org/10.1016/j.foodhyd.2019.105233
930 Wu, Y., Ding, W., & He, Q. (2017). Molecular characteristics of tara galactomannans : Effect of
931 degradation with hydrogen peroxide. *International Journal of Food Properties*, *20*(12),
932 3014-3022. https://doi.org/10.1080/10942912.2016.1270300
933 Xie, Y., Wang, A., Lu, Q., & Hui, M. (2010). The effects of rheological properties of wall materials on
934 morphology and particle size distribution of microcapsule. *Czech Journal of Food Sciences*,
935 *28*(No. 5), 433-439. https://doi.org/10.17221/49/2009-CJFS
936 Yang, Y., & McClements, D. J. (2013). Encapsulation of vitamin E in edible emulsions fabricated using
937 a natural surfactant. *Food Hydrocolloids*, *30*(2), 712-720.
938 https://doi.org/10.1016/j.foodhyd.2012.09.003